

Addressing the Hubble tension with Sterile Neutrino Dark Matter

Debtosh Chowdhury   ^{1,*} Md Sariful Islam   ^{1,†}

¹*Department of Physics, Indian Institute of Technology Kanpur, Kanpur 208016, India*

(Dated: February 16, 2026)

One of the promising dark matter (DM) candidates is a keV scale sterile neutrino. In the early universe the observed relic of the sterile neutrino DM is generated via the *Dodelson-Widrow* mechanism. However, this production scenario is severely constraint by various astrophysical observations. Many non-standard interactions between active (ν_a) and sterile (ν_s) neutrino have been proposed to evade these astrophysical bounds. Here, we study sterile neutrino in the context of a mass-varying scenario by coupling both active and sterile neutrino to a scalar field. This novel mechanism opens up a new parameter space that generates the observed DM relic and alleviates the *Hubble tension*. We find that the resulting parameter space can be fully probed by future X-ray missions.

I. INTRODUCTION

Understanding the fundamental nature of dark matter (DM) remains one of the central open problems in astroparticle physics. Among the proposed candidates, sterile neutrinos with masses in the keV range have received significant attention [1–15]. In the simplest scenario, sterile neutrinos are produced in the early Universe through oscillations with active neutrinos prior to their decoupling and before the onset of Big Bang Nucleosynthesis (BBN). This non-resonant production process is commonly referred to as the *Dodelson-Widrow* (DW) mechanism [1]. Sterile neutrinos are unstable and can undergo radiative decay into an active neutrino accompanied by a photon [16]. Such decays would generate monochromatic X-ray or gamma-ray lines, depending on the sterile neutrino mass, from regions where dark matter is concentrated, such as galaxies and galaxy clusters. However, results from dedicated X-ray and gamma-ray line searches place strong constraints on this scenario, creating significant tension with the DW production mechanism and excluding most of its viable parameter space [17–20].

To evade the experimental bound thus opening up new viable parameter space, many non standard interactions (NSI) have been proposed in DW framework. These NSI can be between active-active ($\nu_a - \nu_a$) neutrino [21, 22] or active-sterile ($\nu_a - \nu_s$) neutrino [23], or sterile-sterile ($\nu_s - \nu_s$) [24, 25] neutrino sector. In the presence of an NSI, new scattering or annihilation channels open up in the active (ν_a) and/or sterile (ν_s) sector. So, the efficient production of the sterile neutrino from the active neutrino happens even for small mixing angle.

Another unsolved problem in modern cosmology is *Hubble tension* (see, e.g., [26, 27] for reviews). The tension arises from the persistent disagreement between determinations of the present-day expansion rate of the

universe, H_0 , inferred from early-universe observations and those obtained from late-universe measurements. Planck satellite measurement of cosmic microwave background(CMB) reported $H_0 = 67.4 \pm 0.5 \text{ km s}^{-1} \text{Mpc}^{-1}$ [28]. In contrast, local distance-ladder measurements based on Cepheid-calibrated Type Ia supernovae from the SH0ES collaboration report a significantly higher value, $H_0 = 73.30 \pm 1.04 \text{ km s}^{-1} \text{Mpc}^{-1}$ [29, 30]. So, there is a 5σ difference between the measured value of H_0 by Planck and SH0ES. To alleviate this tension, many modifications to the Λ CDM cosmology have been proposed [31–33]. One of such solutions is early dark energy (EDE) [34–37]. Refs.[36, 38] studied EDE by quadratically coupling the Standard Model (SM) neutrinos to a background scalar field. Because of this coupling, the ensemble of SM neutrinos i.e., active neutrinos create an effective potential for the scalar but the vacuum expectation value (vev) of the scalar back-reacts and gives active neutrino an effective mass. These effects generate the required dynamics and can address the *Hubble tension*. This tension can also be eased by increasing ΔN_{eff} via the decay of sterile neutrino of mass $\mathcal{O}(30)$ MeV [39] or $\mathcal{O}(150 - 450)$ MeV [40, 41] at BBN.

In this study, we assume that the scalar field now also coupled to the sterile neutrino along with the active neutrino. Hence, the sterile neutrino also gets an effective mass due to the vev of the scalar field. This feature is unique compared to other NSI or lepton-asymmetry model [2] of sterile neutrino. In those models mass of sterile neutrino remains same through out its cosmological history, from production to until today. Whereas, in our case sterile neutrino mass varies as scalar field time evolves. We have shown by increasing the effective sterile mass in early universe we can open a viable parameter space in mixing angle vs. mass plane evading the experimental constraints. We further show that in the allowed region of sterile neutrino parameter space, inferred value of H_0 can be increased and matched with the SH0ES data.

We organized the paper as follows. We setup our model

* debtoshc@iitk.ac.in

† sariful21@iitk.ac.in

in Sec. II and discuss the cosmological evolution of the scalar field and the sterile neutrino in Sec. III. The result is presented in Sec IV and we conclude in Sec. V.

II. MODEL SETUP

In this model, an active neutrino and a sterile neutrino quadratically coupled with a real homogeneous scalar field ϕ . The interaction Lagrangian is given by

$$-\mathcal{L}_{\text{int}} \supset \epsilon \frac{m_{\nu_1}}{M_{\text{pl}}^2} \bar{\nu}_1 \nu_1 \phi^2 + \epsilon \frac{m_{\nu_4}}{M_{\text{pl}}^2} \bar{\nu}_4 \nu_4 \phi^2. \quad (1)$$

Here, ϵ is the coupling strength and M_{pl} is the Planck mass. To ensure that the dimension-five interaction term dominates, we impose a \mathbb{Z}_2 symmetry on the ϕ field and assume its self-interactions are negligible¹ [43]. m_{ν_1} and m_{ν_4} are Dirac masses for active and sterile neutrino, respectively. Sterile and active flavor mixes with each other via a vacuum mixing angle θ . So, we can write sterile and active vacuum mass eigenstate in terms of their flavor eigenstate as

$$\begin{aligned} |\nu_1\rangle &= \cos \theta |\nu_a\rangle - \sin \theta |\nu_s\rangle \\ |\nu_4\rangle &= \cos \theta |\nu_s\rangle + \sin \theta |\nu_a\rangle. \end{aligned} \quad (2)$$

Active and sterile neutrino remain on-shell throughout their cosmological evolution. Therefore, using the equation of motion, effective neutrino masses can be written as [38]

$$\begin{aligned} m_{\nu_1, \text{eff}} &= m_{\nu_1} \left(1 + \epsilon \frac{\phi^2}{M_{\text{pl}}^2} \right) \\ m_{\nu_4, \text{eff}} &= m_{\nu_4} \left(1 + \epsilon \frac{\phi^2}{M_{\text{pl}}^2} \right). \end{aligned} \quad (3)$$

We can see from Eq.(3) that both active and sterile mass scale by same factor because of the universal coupling ϵ . Due to this, vacuum mixing angle θ does not get modified.

The active neutrino remain in thermal equilibrium via the SM weak interactions before BBN. After BBN, it decouples from the thermal plasma with relativistic Fermi-Dirac distribution. As for sterile neutrino, it will never come to thermal equilibrium in our scenario but we can model its phase space density using Fermi-Dirac form [23]

$$f_s(p) = \frac{\alpha}{\exp(p/T_s) + 1}, \quad (4)$$

where T_s is the effective temperature, p is the sterile neutrino momentum and α represents the deviation from the thermal equilibrium with value in the range $0 < \alpha \lesssim 1$. To calculate one-loop effective potential of ϕ , we have used finite temperature correction to the two-point correlation function of ϕ . The effective mass of the scalar field is given by [44, 45]

$$\begin{aligned} m_{\phi, \text{eff}}^2 = & \frac{1}{\phi} \frac{\partial V_{\text{eff}}}{\partial \phi} = \frac{2\epsilon m_{\nu_1}}{M_{\text{pl}}^2} \frac{\rho_{\nu_1} - 3P_{\nu_1}}{m_{\nu_1, \text{eff}}} \\ & + \frac{2\epsilon m_{\nu_4}}{M_{\text{pl}}^2} \frac{\rho_{\nu_4} - 3P_{\nu_4}}{m_{\nu_4, \text{eff}}} + m_{\phi}^2. \end{aligned} \quad (5)$$

In an isotropic and homogeneous expanding universe the evolution of scalar field is governed by

$$\frac{d^2\phi}{dt^2} + 3H(t) \frac{d\phi}{dt} + m_{\phi, \text{eff}}^2 \phi = 0, \quad (6)$$

where t is the proper time and $H(t)$ is the total Hubble rate including contributions from active and sterile neutrinos and the scalar field. We decompose Hubble rate as a sum of Λ CDM part plus the extra contribution due to the finite temperature contribution to ν_1 and ν_4 by the background scalar field. So,

$$H^2 = H_{\Lambda\text{CDM}}^2 + \frac{8\pi}{3M_{\text{pl}}^2} \rho_{\text{extra}}, \quad (7)$$

where ρ_{extra} is

$$\begin{aligned} \rho_{\text{extra}} = & \rho_{\nu_1}(m_{\nu_1, \text{eff}}, T_{\nu_1}) - \rho_{\nu_1}(m_{\nu_1}, T_{\nu_1}) + \\ & \rho_{\nu_4}(m_{\nu_4, \text{eff}}) - \rho_{\text{CDM}} + \frac{1}{2} \left(\frac{d\phi}{dt} \right)^2 + \frac{1}{2} m_{\phi}^2 \phi^2. \end{aligned} \quad (8)$$

Here, $\rho_{\nu_1}(m_{\nu_1, \text{eff}}, T_{\nu_1})$ and $\rho_{\nu_4}(m_{\nu_4, \text{eff}})$ are the modified active and sterile neutrino energy density due to their effective masses, respectively. $\rho_{\nu_1}(m_{\nu_1}, T_{\nu_1})$ is the active neutrino energy density in Λ CDM for $m_{\nu_1} = 0.05$ eV. ρ_{CDM} is the cold dark matter energy density. As $\rho_{\nu_1}(m_{\nu_1}, T_{\nu_1})$ and ρ_{CDM} are included in $H_{\Lambda\text{CDM}}$, we subtracted them in Eq.(8).

The production of sterile neutrinos proceeds via oscillations between active and sterile neutrino states in the early universe, prior to Big Bang Nucleosynthesis (BBN), through the so-called Dodelson–Widrow mechanism [1]. The evolution of the sterile neutrino phase-space distribution is described by a semi-classical Boltzmann equation of the form [3, 4, 46–49]

¹ For the effect of the quartic self-interaction term of the scalar field on the Hubble tension see Ref.[42].

$$\frac{\partial}{\partial t} f_s(p, t) - H p \frac{\partial}{\partial p} f_s(p, t) \approx \frac{1}{4} \frac{\Gamma_a(p) \Delta^2(p) \sin^2 2\theta}{\Delta^2(p) \sin^2 2\theta + (\Gamma_a(p))^2 / 4 + [\Delta(p) \cos 2\theta - V_T]^2} \times [f_a(p, t) - f_s(p, t)], \quad (9)$$

where $f_s(p, t)$ denotes sterile neutrino distribution function, $f_a(p, t)$ is the active neutrino Fermi-Dirac distribution function, $\Delta(p) = \frac{m_{\nu_4, \text{eff}}^2 - m_{\nu_1, \text{eff}}^2}{2p}$, and $\Gamma_a(p)$ is the active neutrino forward interaction rate. The effective matter-mixing angle is given by

$$\sin^2 2\theta_m = \frac{\Delta^2(p) \sin^2 2\theta}{\Delta^2(p) \sin^2 2\theta + [\Delta(p) \cos 2\theta - V_T]^2}. \quad (10)$$

In SM, $\Gamma_a(p)$ is obtained by summing over all leptonic and hadronic channels as [4, 50, 51]

$$\Gamma_a(p) = C_a(T) G_F^2 p T^4, \quad (11)$$

where $C_a(T)$ is a temperature-dependent function. We have numerically evaluated the value of $\Gamma_a(p)$ from [52]. The SM thermal potential V_T is [53–55]

$$V_T(p) = -\frac{8\sqrt{2}G_F p}{3m_W^2} (\rho_{l_a} + \rho_{\bar{l}_a}) - \frac{8\sqrt{2}G_F p}{3m_Z^2} (\rho_{\nu_a} + \rho_{\bar{\nu}_a}), \quad (12)$$

where $\rho_{l_a}/\rho_{\bar{l}_a}$ is the energy density of charged lepton (l_a)/antilepton (\bar{l}_a) with flavor a as active neutrino, and p is the active neutrino momentum. The non-standard interaction (NSI) terms are suppressed by M_{pl}^2 . So, the scattering channel $\nu_a \nu_s \leftrightarrow \nu_a \nu_s$ or annihilation channel $\nu_a \nu_a \leftrightarrow \nu_s \nu_s$ will be highly suppressed compared to SM weak interaction channels (i.e., $\nu_a + \nu_a \leftrightarrow \nu_a + \nu_a, l_a + \nu_a \leftrightarrow l_a + \nu_a$ etc). Hence, the contribution due to the NSI terms in $\Gamma_a(p)$ or V_T are highly suppressed.

III. COSMOLOGICAL EVOLUTION

In the early universe at some high temperature ($T \gtrsim 100$ GeV), ϕ field is displaced from the minimum of its potential to some value ϕ_0 , close to the Planck scale. This displacement of the scalar field will come from some UV dynamics. Since $H^2 \gg m_{\phi, \text{eff}}^2$, at this time the evolution equation of ϕ , Eq.(6) is highly overdamped, leaving the scalar frozen at ϕ_0 (see Fig. 1). So, the effective mass of the sterile neutrino becomes constant at this time, $m_{\nu_4, \text{eff}}^{\text{max}} = m_{\nu_4} \left(1 + \epsilon \frac{\phi_0^2}{M_{\text{pl}}^2}\right)$. For a given ϵ and ϕ_0 , $m_{\nu_4, \text{eff}}^{\text{max}}$ is the maximum effective mass of the sterile neutrino. With this enhanced effective mass sterile neutrino starts to produce. We calculate the yield (Y_{ν_4}) of the sterile neutrino dark matter by numerically solving Eq.(9) after modifying publicly available **sterile-dm** code [52]. In Fig. 2 we show evolution of Y_{ν_4} from temperature ranging from 50 GeV to 10 MeV for present day sterile mass, $m_{\nu_4} = 10$ keV. From blue to green line early universe sterile mass, $m_{\nu_4, \text{eff}}^{\text{max}}$ changes from 10 MeV to 1 GeV. We observe from

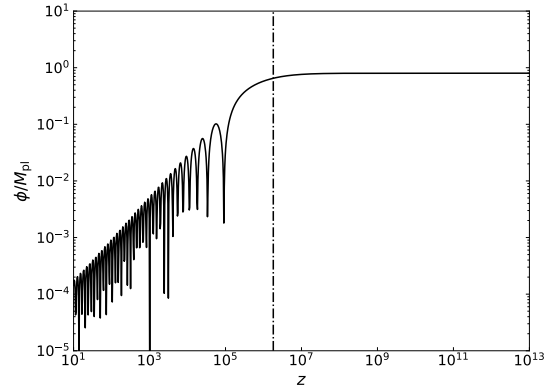


FIG. 1: Evolution of the scalar field for $\phi_0/M_{\text{pl}} = 0.8$ and coupling, $\epsilon = 1.56 \times 10^3$. Here, sterile neutrino mass is 10 keV and effective mass is 10 MeV. The vertical line is at $z_{\text{osc}} = 1.81 \times 10^6$.

Fig. 2 increasing $m_{\nu_4, \text{eff}}^{\text{max}}$ leads to production of the sterile neutrino at increasingly high temperature. This happens because increasing the $m_{\nu_4, \text{eff}}^{\text{max}}$ increases the $\Delta(p)$. So, $\Delta(p)$ dominates over thermal potential(V_T) even at large temperature. Therefore, matter-mixing angle of the sterile neutrino is no longer suppressed (see Eq.(10)). These effects lead to enhanced production of sterile neutrino at high temperature. The maximum of sterile neutrino production occurs at temperature [1]

$$T_{\text{max}} \approx 133 \text{ MeV} \left(\frac{m_{\nu_4, \text{eff}}^{\text{max}}}{1 \text{ keV}} \right)^{1/3}. \quad (13)$$

For $T \gg T_{\text{max}}$, thermal potential V_T dominates over $\Delta(p)$. Hence, from Eq.(9) we see that $Y_{\nu_4} \propto \left(m_{\nu_4, \text{eff}}^{\text{max}}\right)^4 \sin^2(2\theta)/T^9$. At $T \ll T_{\text{max}}$, sterile co-moving number density freezes out and yield Y_{ν_4} becomes constant until today. The freeze out happens by the time of BBN in our parameter space. The relic can then be computed as $\Omega_{\text{DM}} = Y_{\nu_4,0} s_0 m_{\nu_4} / \rho_0$ where s_0 and ρ_0 is the entropy density and critical energy density today respectively. $Y_{\nu_4,0}$ is the sterile neutrino yield at today. Then from Eq.(13),

$$\Omega_{\text{DM}} \propto m_{\nu_4, \text{eff}}^{\text{max}} m_{\nu_4} \sin^2(2\theta). \quad (14)$$

Therefore, to satisfy the DM relic $\omega_{\text{DM}} = \Omega_{\text{DM}} h^2 = 0.12$, we can accommodate less mixing between active and sterile neutrino for a given m_{ν_4} by increasing $m_{\nu_4, \text{eff}}^{\text{max}}$. From Fig. 2, we see that changing $m_{\nu_4, \text{eff}}^{\text{max}}$ by one order will reduce $\sin^2 2\theta$ by one order for a fixed m_{ν_4} .

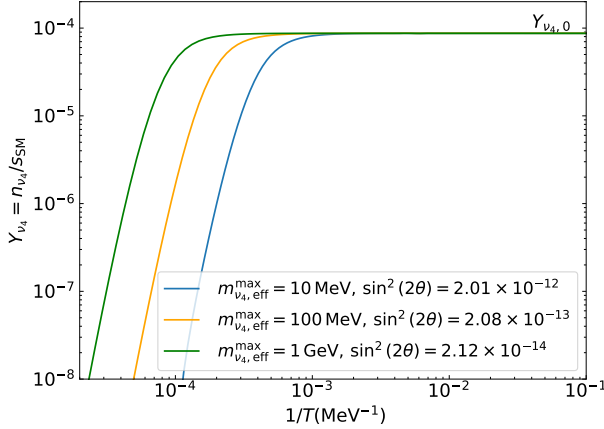


FIG. 2: Yield of sterile neutrino for present day sterile mass of $m_{\nu_4} = 10 \text{ keV}$. Increasing $m_{\nu_4, \text{eff}}^{\text{max}}$ by one order leads to production at higher temperature and reduce vacuum mixing angle by one order.

The ϕ starts oscillating when effective potential of the scalar dominates over the Hubble friction term i.e., $m_{\phi, \text{eff}}^2 \gg H^2$. Active neutrinos are relativistic during their evolution i.e., $P_{\nu_1} \approx \frac{1}{3} \rho_{\nu_1}$. As for m_{ϕ} , it should be $m_{\phi} \lesssim H(z_{\text{CMB}}) \approx 10^{-29} \text{ eV}$ such that the ϕ decays by the time of CMB and does not have a significant contribution to the Hubble parameter. Therefore, we set $m_{\phi} = 0$ for numerical analysis. So, from Eq.(5) we see that in $m_{\phi, \text{eff}}^2$ sterile neutrino mostly contributes. Sterile neutrino becomes non-relativistic close to BBN in our scenario of interest. Hence, ignoring pressure term for sterile neutrino in Eq.(5) the redshift at which the scalar field starts oscillating is determined by equating $m_{\phi, \text{eff}}^2 = H^2$ as

$$z_{\text{osc}} \simeq \frac{3 \epsilon \omega_{\text{DM}}}{4 \pi \omega_{\text{rad}}}, \quad (15)$$

where ω_{DM} and ω_{rad} is the present day relic density of DM and radiation respectively. In deriving Eq.(15) we have assumed oscillation happens during radiation domination. The value of z_{osc} (vertical dashed line) is of the order of 10^6 from Fig. 1. Amplitude of the oscillation of ϕ is calculated using WKB approximation as [43]

$$\phi_{\text{amp}} \propto \left(\frac{1}{\phi} \frac{\partial V_{\text{eff}}}{\partial \phi} \right)^{-1/4} (1+z)^{3/2} \propto (1+z)^{3/4}. \quad (16)$$

Hence, the kinetic energy density of the scalar field redshifts away as $\frac{1}{2} \left(\frac{d\phi}{dt} \right)^2 \propto (1+z)^{11/2}$ in RD and $\frac{1}{2} \left(\frac{d\phi}{dt} \right)^2 \propto (1+z)^{9/2}$ during MD faster than any other component of the universe. So, scalar field will not have any relic in the present time.

The non-trivial evolution of ρ_{ν_4} happens during the oscillation of ϕ field. From Eqs.(3) and (16), the effective sterile mass hence energy density redshifts as $\rho_{\nu_4} \propto (1+z)^{9/2}$

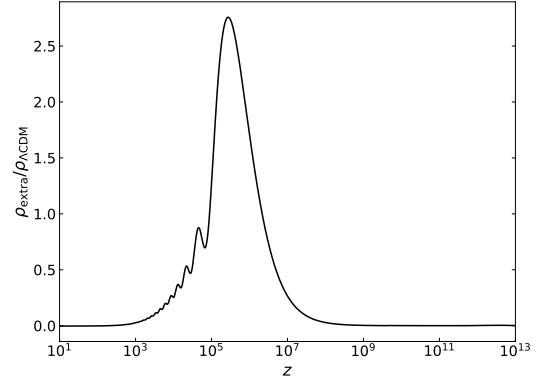


FIG. 3: Evolution of extra energy density (ρ_{extra}) as a ratio of ρ_{ν_4} to $\rho_{\Lambda \text{CDM}}$ for $\phi_0/M_{\text{Pl}} = 0.8$ and coupling, $\epsilon = 1.56 \times 10^3$.

Here, present day sterile neutrino mass is 10 keV and effective mass is 10 MeV. ρ_{extra} has of the order $\rho_{\Lambda \text{CDM}}$ contribution in the redshift range $z \approx 10^7 - 10^3$.

during this epoch. We can summarize the evolution of ρ_{ν_4} as follows

$$\rho_{\nu_4} \propto \begin{cases} m_{\nu_4} \epsilon \frac{\phi_0^2}{M_{\text{Pl}}^2} (1+z)^3, & z > z_{\text{osc}} \\ m_{\nu_4} \epsilon \frac{\phi_0^2}{M_{\text{Pl}}^2} (1+z)^{9/2}, & z_{\text{decay}} < z < z_{\text{osc}} \\ m_{\nu_4} (1+z)^3, & z < z_{\text{decay}} \end{cases} \quad (17)$$

where $z_{\text{decay}} = \left(10^{-2} \times \frac{M_{\text{Pl}}^2}{\epsilon \phi_0^2} \right)^{2/3} \times z_{\text{osc}}$ is the redshift value when effective sterile mass returns to present day sterile mass within 1%. We see from Eq.(17), before the oscillation of the ϕ field sterile energy density is greater than ΛCDM cold dark matter density by a factor of $\epsilon \frac{\phi_0^2}{M_{\text{Pl}}^2}$. So, in the early universe total energy density hence Hubble value will be larger than ΛCDM .

We show how this extra contribution changes with redshift in Fig. 3. Between the redshift $10^7 - 10^3$, ρ_{extra} has a significant contribution of the order of $\rho_{\Lambda \text{CDM}}$. This extra energy density before photon decoupling changes the sound horizon at the surface of last scattering. This in turns alter inferred value of H_0 . The change in H_0 can be estimated as [34, 38]

$$1 + \frac{\delta H_0}{H_0} \approx \frac{\int_{z_{\text{CMB}}}^{\infty} dz (\rho_{\Lambda \text{CDM}} (1+R(z)))^{-1/2}}{\int_{z_{\text{CMB}}}^{\infty} dz ((\rho_{\Lambda \text{CDM}} + \rho_{\text{extra}}) (1+R(z)))^{-1/2}} \times \frac{\int_0^{z_{\text{CMB}}} dz (\rho_{\Lambda \text{CDM}} + \rho_{\text{extra}})^{-1/2}}{\int_0^{z_{\text{CMB}}} dz (\rho_{\Lambda \text{CDM}})^{-1/2}}, \quad (18)$$

where $R(z) = \frac{3}{4} \frac{\omega_b}{\omega_{\gamma}} (1+z)^{-1}$ and $\omega_b = 2.24 \times 10^{-2}$, $\omega_{\gamma} = 2.47 \times 10^{-5}$ are the present day baryon and photon ΛCDM relic densities. We have taken the redshift of recombination $z_{\text{CMB}} = 1080$ and ΛCDM 's H_0 central value equals to $67.4 \text{ km s}^{-1} \text{ Mpc}^{-1}$.

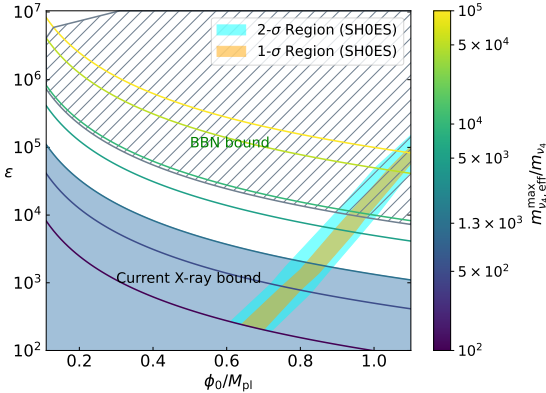


FIG. 4: Scalar field parameter space for $m_{\nu_4} = 10$ keV. Each contour line corresponds to different $m_{\nu_4, \text{eff}}^{\text{max}}/m_{\nu_4}$ and satisfies the DM relic, $\Omega_{\text{DM}} h^2 = 0.12$ for specific values of $\sin^2 2\theta$. H_0 value increases when we go left to right along each contour. We have marked SH0ES 1- σ and 2- σ regions by orange and cyan color respectively. Below $m_{\nu_4, \text{eff}}^{\text{max}}/m_{\nu_4} = 1.3 \times 10^3$ marked by steelblue shaded region is excluded by X-ray observations. Above $m_{\nu_4, \text{eff}}^{\text{max}}/m_{\nu_4} = 8.8 \times 10^3$ hatched region is excluded by BBN.

IV. RESULTS

We delineate the parameter space for the scalar field ϕ in Fig. 4. In each contour line $m_{\nu_4, \text{eff}}^{\text{max}}/m_{\nu_4}$ is constant with $m_{\nu_4} = 10$ keV. Each contour will satisfy the DM relic for a specific value of $\sin^2 2\theta$. We reduce the mixing angle by increasing the ratio of $m_{\nu_4, \text{eff}}^{\text{max}}/m_{\nu_4}$. For example, $m_{\nu_4, \text{eff}}^{\text{max}}/m_{\nu_4} = 10^3, 10^4$ satisfy relic for $\sin^2 2\theta = 2.01 \times 10^{-12}, 2.08 \times 10^{-13}$ respectively. In this way sterile neutrino evade the bound coming from X-ray observations by allowing smaller mixing angle. Along each contour when we go left to right ϕ_0 increases but ϵ decreases. Therefore, from Eq.(15) z_{osc} value also decreases. So, the oscillation of scalar field begins at later time. Consequently, ρ_{extra} contributes more to the total energy density at later times especially close to matter-radiation equality(MRE). Hence, H_0 value increases and can be matched with SH0ES value 73.04 ± 1.04 km/s/Mpc thus solving hubble tension in a certain region of $\epsilon - \phi_0$ space. We delineate SH0ES 1- σ and 2- σ regions by orange and cyan color respectively in Fig. 4.

From publicly available code `alterbbn` [56, 57], maximum allowed extra DM energy density at the time of BBN ($T = 1$ MeV) is 10^{-2} times the photon density at BBN. DM densities larger than this value are excluded at the 2σ (95% C.L.) level by BBN constraints from the primordial helium mass fraction Y_p and the deuterium-to-hydrogen ratio $\left(\frac{D}{H}\right)_p$. The value of Y_p is taken to be 0.245 ± 0.003 [58–64]. We have taken

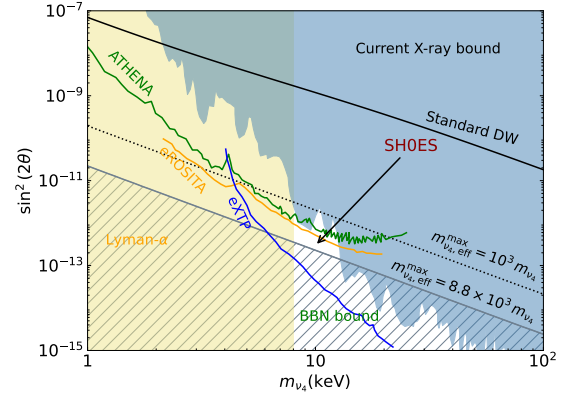


FIG. 5: Sterile neutrino parameter space in presence of our new interaction term. In the white region DM relic and Hubble tension both can be satisfied. The black dotted and gray solid lines correspond to relic line for $m_{\nu_4, \text{eff}}^{\text{max}}/m_{\nu_4} = 10^3$ and 8.8×10^3 respectively. X-ray and Lyman- α bounds are denoted by steelblue and light yellow region respectively. The sensitivity curves of future X-ray missions [23] are shown in green(ATHENA), in blue(eXTP), and in orange(eROSITA). The black solid line is the standard Dodelson-Widrow line.

$\left(\frac{D}{H}\right)_p = (25.47 \pm 0.29) \times 10^{-6}$ [58, 65–71]. In Λ CDM the ratio of DM density to photon density at BBN ($T = 1$ MeV) is of the order of 10^{-6} . In our scenario, sterile neutrino DM has $m_{\nu_4, \text{eff}}^{\text{max}}/m_{\nu_4}$ more density compared to Λ CDM at BBN from Eq.(17). So, maximum allowed value of $m_{\nu_4, \text{eff}}^{\text{max}}/m_{\nu_4}$ at BBN is 8.8×10^3 . We represent this bound by hatched region in Fig. 4. To evade this BBN bound we can decay the scalar field before BBN by increasing the coupling such that z_{osc} becomes greater than redshift of BBN. In Fig. 4 in the white region at top left corner, the decay of ϕ happens before BBN. But for this values of ϵ and ϕ_0 the *Hubble tension* cannot be alleviated for any m_{ν_4} .

We depict the sterile neutrino parameter space in $\sin^2 2\theta - m_{\nu_4}$ space in Fig. 5. The solid black line is the Dodelson-Widrow line corresponding to no new non-standard interactions. In presence of new interaction given in Eq.(1) viable parameter space is opened up without violating current X-ray bounds from Chandra [17], XMM-Newton [18], NuSTAR [19], and XRISM [20] telescopes. The X-ray constraint is marked by steelblue region. The black dotted line and gray solid line corresponds to relic line for $m_{\nu_4, \text{eff}}^{\text{max}}/m_{\nu_4} = 10^3$ and 8.8×10^3 respectively. As noted earlier, the more we increase $m_{\nu_4, \text{eff}}^{\text{max}}/m_{\nu_4}$ ratio the less mixing we need between active and sterile sector. The hatched region in Fig. 5 is excluded by BBN. In the white region of Fig. 5 we can solve the *Hubble tension*. Following reference [23] we also add future sensitivities of upcoming missions of ATHENA (green line) [72], eROSITA (orange line) [73],

and eXTP (blue line) [74]. The parameter region of interest lies in the sweet spot of sensitivities of future missions. Lyman- α forest imposes a mass bound of $m_{\nu_4} \gtrsim 8$ keV considering suppression of matter power spectrum in small-scale structures by relatively large free-streaming length of the sterile neutrino. This constraint is marked by light yellow region in Fig. 5.

V. CONCLUSION

We have studied the production of sterile neutrino dark matter before BBN via the *Dodelson-Widrow* (DW) mechanism in the presence of a new interaction term given in Eq.(1). This interaction universally couples sterile and active neutrino to a real homogeneous scalar field (ϕ) quadratically and generated the observed relic. The scalar field gives an effective mass ($m_{\nu_4, \text{eff}}$) to the sterile neutrino. Due to this enhanced effective mass, production of the sterile neutrino from the active neutrino happens at high temperature. This results in a smaller vacuum mixing angle ($\sin^2 2\theta$) needed for the DM relic generation compared to DW scenario. We have used this feature to allow a smaller $\sin^2 2\theta$ by increasing $m_{\nu_4, \text{eff}}^{\text{max}}$ in the parameter space of the sterile neutrino. In standard DW scenario this region of smaller $\sin^2 2\theta$ yields a under abundant DM relic.

Besides that, we have demonstrated that *Hubble tension* can be alleviated in this region of parameter space of the sterile neutrino for a suitable choice of coupling (ϵ) and initial value of the scalar field (ϕ_0). This happens because

energy density of the sterile neutrino DM has $m_{\nu_4, \text{eff}}/m_{\nu_4}$ times more contribution compared to the energy density of DM in the Λ CDM cosmology. So, the Hubble parameter before recombination increases leading to a smaller sound horizon at the last scattering surface of the CMB. Hence, inferred value of the present day Hubble parameter (H_0) increases.

Also an increased Hubble rate during BBN leads to a larger neutron-to-proton ratio at freeze-out, thereby enhancing the primordial helium and deuterium abundances beyond observational limits [58]. The corresponding constraint on $\sin^2 2\theta$ translates into a relic-density contour defined by $m_{\nu_4, \text{eff}}^{\text{max}}/m_{\nu_4} = 8.8 \times 10^3$.

After considering the astrophysical constraints, Lyman- α forest bound, and BBN bound, sterile neutrino mass (m_{ν_4}) in the range 8-10 keV and vacuum mixing angle ($\sin^2 2\theta$) in the range $10^{-12} - 10^{-13}$ satisfies successfully the SH0ES result (white region in Fig. 5). Interestingly, this region can be fully explored by upcoming missions such as ATHENA [72], eROSITA [73], eXTP [74].

ACKNOWLEDGMENTS

We thank Srubabati Goswami and Navaneeth Poonthotathil for helpful discussions. D.C. acknowledge funding from the ANRF, Government of India, under grant ANRF/CRG/2021/007579. M.S.I would like to thank the MHRD, Govt. of India for the research fellowship. D.C. also acknowledges support from an initiation grant IITK/PHY/2019413 at IIT Kanpur and funding from the Indian Space Research Organisation (ISRO) under grant STC/PHY/2024427Q.

[1] S. Dodelson and L. M. Widrow, *Physical Review Letters* **72**, 17 (1994).

[2] X.-D. Shi and G. M. Fuller, *Phys. Rev. Lett.* **82**, 2832 (1999), arXiv:astro-ph/9810076.

[3] A. D. Dolgov and S. H. Hansen, *Astroparticle Physics* **16**, 339 (2002), arXiv:hep-ph/0009083 [hep-ph].

[4] K. Abazajian, G. M. Fuller, and M. Patel, *Phys. Rev. D* **64**, 023501 (2001), arXiv:astro-ph/0101524.

[5] K. Abazajian, G. M. Fuller, and W. H. Tucker, *The Astrophysical Journal* **562**, 593 (2001), arXiv:astro-ph/0106002 [astro-ph].

[6] T. Asaka, S. Blanchet, and M. Shaposhnikov, *Physics Letters B* **631**, 151 (2005), arXiv:hep-ph/0503065 [hep-ph].

[7] T. Asaka and M. Shaposhnikov, *Physics Letters B* **620**, 17 (2005), arXiv:hep-ph/0505013 [hep-ph].

[8] M. Shaposhnikov and I. Tkachev, *Physics Letters B* **639**, 414 (2006), arXiv:hep-ph/0604236 [hep-ph].

[9] A. Kusenko, *Physical Review Letters* **97**, 241301 (2006), arXiv:hep-ph/0609081 [hep-ph].

[10] K. Petraki and A. Kusenko, *Physical Review D* **77**, 065014 (2008), arXiv:0711.4646 [hep-ph].

[11] K. Petraki, *Physical Review D* **77**, 105004 (2008), arXiv:0801.3470 [hep-ph].

[12] M. Loewenstein, A. Kusenko, and P. L. Biermann, *The Astrophysical Journal* **700**, 426 (2009), arXiv:0812.2710 [astro-ph].

[13] M. Loewenstein and A. Kusenko, *The Astrophysical Journal* **714**, 652 (2010), arXiv:0912.0552 [astro-ph.CO].

[14] M. Drewes *et al.*, *Journal of Cosmology and Astroparticle Physics* **2017** (01), 025, arXiv:1602.04816 [hep-ph].

[15] A. Merle, *PoS NOW2016*, 082 (2017), arXiv:1702.08430 [hep-ph].

[16] P. B. Pal and L. Wolfenstein, *Physical Review D* **25**, 766 (1982).

[17] F. Hofmann, J. S. Sanders, K. Nandra, N. Clerc, and M. Gaspari, *Astron. Astrophys.* **592**, A112 (2016), arXiv:1606.04091 [astro-ph.CO].

[18] E. Borriello, M. Paolillo, G. Miele, G. Longo, and R. Owen, *Mon. Not. Roy. Astron. Soc.* **425**, 1628 (2012), arXiv:1109.5943 [astro-ph.GA].

[19] R. A. Krivonos, V. V. Barinov, A. A. Mukhin, and D. S. Gorbunov, *Phys. Rev. Lett.* **133**, 261002 (2024), arXiv:2405.17861 [hep-ph].

[20] W. Yin, Y. Fujita, Y. Ezoe, and Y. Ishisaki, (2025), arXiv:2503.04726 [hep-ph].

[21] A. De Gouv  a, M. Sen, W. Tangarife, and Y. Zhang, Phys. Rev. Lett. **124**, 081802 (2020), arXiv:1910.04901 [hep-ph].

[22] K. J. Kelly, M. Sen, W. Tangarife, and Y. Zhang, Phys. Rev. D **101**, 115031 (2020), arXiv:2005.03681 [hep-ph].

[23] P. S. Bhupal Dev, B. Dutta, S. Goswami, J. P. Tang, and A. Ujjayini Ramachandran, arXiv e-prints , arXiv:2505.22463 (2025).

[24] M. D. Astros and S. Vogl, JHEP **03**, 032, arXiv:2307.15565 [hep-ph].

[25] T. Bringmann, P. F. Depta, M. Hufnagel, J. Kersten, J. T. Ruderman, and K. Schmidt-Hoberg, Phys. Rev. D **107**, L071702 (2023), arXiv:2206.10630 [hep-ph].

[26] E. Di Valentino *et al.*, Class. Quant. Grav. **38**, 153001 (2021).

[27] A. R. Khalife *et al.*, J. Cosmol. Astropart. Phys. **2024** (04), 059.

[28] N. Aghanim *et al.* (Planck), Astron. Astrophys. **641**, A6 (2020), [Erratum: Astron.Astrophys. 652, C4 (2021)], arXiv:1807.06209 [astro-ph.CO].

[29] A. G. Riess *et al.*, Astrophys. J. **826**, 56 (2016), arXiv:1604.01424 [astro-ph.CO].

[30] A. G. Riess *et al.*, Astrophys. J. Lett. **934**, L7 (2022), arXiv:2112.04510 [astro-ph.CO].

[31] T. L. Smith, V. Poulin, and M. A. Amin, Phys. Rev. D **101**, 063523 (2020).

[32] G. Benevento, W. Hu, and M. Raveri, Phys. Rev. D **101**, 103517 (2020).

[33] T. Clifton and N. Hyatt, J. Cosmol. Astropart. Phys. **2024** (08), 052.

[34] M. Kamionkowski and A. G. Riess, Ann. Rev. Nucl. Part. Sci. **73**, 153 (2023), arXiv:2211.04492 [astro-ph.CO].

[35] T. Karwal and M. Kamionkowski, Phys. Rev. D **94**, 103523 (2016).

[36] J. Sakstein and M. Trodden, Phys. Rev. Lett. **124**, 161301 (2020).

[37] V. Poulin, T. L. Smith, T. Karwal, and M. Kamionkowski, Phys. Rev. Lett. **122**, 221301 (2019).

[38] M. Kamionkowski and A. Mathur, Phys. Rev. D **111**, 063551 (2025).

[39] G. B. Gelmini, A. Kusenko, and V. Takhistov, J. Cosmol. Astropart. Phys. **2021** (06), 002.

[40] G. B. Gelmini, M. Kawasaki, A. Kusenko, K. Murai, and V. Takhistov, J. Cosmol. Astropart. Phys. **2020** (09), 051.

[41] A. D. Dolgov, S. H. Hansen, G. Raffelt, and D. V. Semikoz, Nuclear Physics B **590**, 562 (2000), arXiv:hep-ph/0008138 [hep-ph].

[42] J. N. L  pez-S  nchez, arXiv (2025), arXiv:2512.24309 [astro-ph.CO].

[43] S. Sibiryakov, P. S  rensen, and T.-T. Yu, JHEP **2020** (12), 075, arXiv:2006.04820 [hep-ph].

[44] T. Bouley, P. S  rensen, and T.-T. Yu, JHEP **03**, 104, arXiv:2211.09826 [hep-ph].

[45] A. Y. Smirnov and X.-J. Xu, JHEP **08**, 170, arXiv:2201.00939 [hep-ph].

[46] L. Stodolsky, Phys. Rev. D **36**, 2273 (1987).

[47] R. Foot and R. R. Volkas, Phys. Rev. D **55**, 5147 (1997).

[48] P. Di Bari, P. Lipari, and M. Lusignoli, Int. J. Mod. Phys. A **15**, 2289 (2000), arXiv:hep-ph/9907548.

[49] K. S. M. Lee, R. R. Volkas, and Y. Y. Y. Wong, Phys. Rev. D **62**, 093025 (2000).

[50] T. Asaka, M. Laine, and M. Shaposhnikov, JHEP **01**, 091, [Erratum: JHEP 02, 028 (2015)], arXiv:hep-ph/0612182.

[51] A. Merle, A. Schneider, and M. Totzauer, Journal of Cosmology and Astroparticle Physics (04), 003–003.

[52] T. Venumadhav, F.-Y. Cyr-Racine, K. N. Abazajian, and C. M. Hirata, Phys. Rev. D **94**, 043515 (2016).

[53] D. N  tzold and G. Raffelt, Nucl. Phys. B **307**, 924 (1988).

[54] K. Abazajian, Phys. Rev. D **73**, 063506 (2006).

[55] J. C. D’Olivo, J. F. Nieves, and M. Torres, Phys. Rev. D **46**, 1172 (1992).

[56] A. Arbey, Comput. Phys. Commun. **183**, 1822 (2012), arXiv:1106.1363 [astro-ph.CO].

[57] A. Arbey, J. Auffinger, K. P. Hickerson, and E. S. Jenssen, Comput. Phys. Commun. **248**, 106982 (2020), arXiv:1806.11095 [astro-ph.CO].

[58] S. Navas *et al.* (Particle Data Group), Phys. Rev. D **110**, 030001 (2024).

[59] E. Aver, D. A. Berg, K. A. Olive, R. W. Pogge, J. J. Salzer, and E. D. Skillman, Journal of Cosmology and Astroparticle Physics **2021** (03), 027, arXiv:2010.04180 [astro-ph.CO].

[60] M. Valerdi, A. Peimbert, M. Peimbert, and A. Sixtos, The Astrophysical Journal **876**, 98 (2019).

[61] V. Fern  ndez, E. Terlevich, A. I. D  az, and R. Terlevich, Mon. Not. R. Astron. Soc. **487**, 3221 (2019).

[62] O. A. Kurichin, P. A. Kislytsyn, V. V. Klimenko, S. A. Balashev, and A. V. Ivanchik, Mon. Not. R. Astron. Soc. **502**, 3045 (2021).

[63] T. Hsyu, R. J. Cooke, J. X. Prochaska, and M. Bolte, Astrophys. J. **896**, 77 (2020).

[64] M. Valerdi, A. Peimbert, and M. Peimbert, Mon. Not. R. Astron. Soc. **505**, 3624 (2021).

[65] R. J. Cooke, M. Pettini, R. A. Jorgenson, M. T. Murphy, and C. C. Steidel, The Astrophysical Journal **781**, 31 (2014), arXiv:1308.3240 [astro-ph.CO].

[66] R. J. Cooke, M. Pettini, K. M. Nollett, and R. A. Jorgenson, The Astrophysical Journal **830**, 148 (2016), arXiv:1607.03900 [astro-ph.CO].

[67] S. Riemer-S  rensen, J. K. Webb, N. H. M. Crighton, V. Dumont, K. Ali, S. Kotus, M. Bainbridge, M. T. Murphy, and R. F. Carswell, Monthly Notices of the Royal Astronomical Society **447**, 2925 (2015), arXiv:1412.4043 [astro-ph.CO].

[68] S. A. Balashev, E. O. Zavarygin, A. V. Ivanchik, K. N. Telikova, and D. A. Varshalovich, Monthly Notices of the Royal Astronomical Society **458**, 2188 (2016), arXiv:1511.01797 [astro-ph.CO].

[69] S. Riemer-S  rensen, S. Kotus, J. K. Webb, K. Ali, V. Dumont, M. T. Murphy, and R. F. Carswell, Monthly Notices of the Royal Astronomical Society **468**, 3239 (2017).

[70] E. O. Zavarygin, J. K. Webb, V. Dumont, and S. Riemer-S  rensen, in *Journal of Physics: Conference Series*, Vol. 1038 (2018) p. 012012, arXiv:1801.04704 [astro-ph.CO].

[71] R. J. Cooke, M. Pettini, and C. C. Steidel, The Astrophysical Journal **855**, 102 (2018), arXiv:1710.11129 [astro-ph.CO].

[72] D. Barret, A. Decourchelle, A. Fabian, M. Guainazzi, K. Nandra, R. Smith, and J.-W. d. Herder, Astron. Nachr. **341**, 224 (2020), arXiv:1912.04615 [astro-ph.IM].

[73] A. Merloni *et al.* (eROSITA), (2012), arXiv:1209.3114 [astro-ph.HE].

[74] D. Malyshev, C. Thorpe-Morgan, A. Santangelo, J. Jochum, and S.-N. Zhang, *Phys. Rev. D* **101**, 123009 (2020), arXiv:2001.07014 [astro-ph.HE].